



CLUSTER RADIOACTIVITY IN ^{287}Mc USING MODIFIED GENERALIZED LIQUID DROP MODEL

N. Manjunatha*¹, A.M. Nagaraja^{1,3}, N. Sowmya¹, H.C. Manjunatha*¹, P.S. Damodara Gupta¹,
L. Seenappa¹, K.N.Sridhar², S. Alfred Cecil Raj³

¹Department of Physics, Government College for Women, Kolar, Karnataka, India

²Department of Physics, Government First Grade College, Kolar, Karnataka, India

³Department of Physics, St. Joseph's college (Autonomous), Affiliated to Bharathidasan University, Tiruchirappalli, Tamil Nadu, India

*Corresponding author: manjunathhc@rediffmail.com

ABSTRACT

Using modified generalized liquid drop model, we have studied all possible cluster decay modes of superheavy nuclei ^{287}Mc using different nuclear potentials. The daughter or residual nuclei is having magic nuclei or semi-magic nuclei. The total potential is evaluated by considering quantum tunneling process. The lower limit of cluster emission is from $Z_e^{\min} = 2$ and upper limit of cluster emission considered is $Z_e^{\max} = Z - 82$. The studied different nuclear potentials such as Danisov, AW-91, BW-91 and Bass-73 shows shorter half-lives and larger relative yield for the cluster emission ^{74}Ge . Hence, the possible cluster decay is with the combination $^{74}\text{Ge} + ^{213}\text{Bi}$.

Keywords: Cluster decay, Quantum tunneling, Superheavy element, Half-lives.

1. INTRODUCTION

As a first attempt to synthesize a transuranic element heavier than Uranium, a group of Italian scientists led by Enrico Fermi bombarded uranium nuclei with free neutrons in 1934. Neptunium was the first such element to be synthesized, with an atomic number of 93. Since then, several new elements have been synthesised in the lab, and their properties have been studied. Hot fusion reactions with ^{48}Ca projectiles produced three new elements with the atomic numbers 114, 116, and 118. Denisov and Hofmann [1] investigated shell structure and nuclear stability of the projectile and target combination using cold fusion reactions. Brodzinski and Skalski [2] theoretically predicted fission half-lives of superheavy element $Z=128-148$ using microscopic-macroscopic models. Using preformation cluster model, Wei and Zhang [3] studied an alpha and cluster radioactivity in the heavy and superheavy nuclei. To provide insight into the physics of cold-fusion reactions leading to the formation of elements at the end of the periodic system, Takatoshi Ichikawa [4] assumed that the target and projectile remain spherical during the collision and that the barrier can be described as a sum of Coulomb interaction and a short-range nuclear interaction. The experiments described by Oganessian [5] were targeted at producing nuclides with $Z = 113-$

116, 118, and $N = 170-177$ in the fusion reactions of heavy isotopes of Pu, Am, Cm and Cf with ^{48}Ca projectiles. Using the Cubic plus Yukawa Plus Exponential Model in two sphere approximations and including parent deformation and parent cluster deformations [6], computed the heavy cluster radioactivity half-lives of some of the set of isotopes of Superheavy nuclei. The values of the preformation factors were calculated using the experimental cluster decay half-lives, assuming that the heavy-ion emission decay constant equals the product of the assault frequency, the preformation factor, and the penetrability. D.N. Poenaru and R.A. Gherghescu [7] described the analytical superasymmetric fission (ASAF) model, which is widely used to forecast the half-lives of heavy and superheavy ($Z > 104$) elements. For the 26 cluster decays that have already been measured (from ^{14}C to $^{32,34}\text{Si}$ of parent nuclides with $Z = 87-96$). The Skyrem-Hartree-Fock method with a density-independent contact pairing interaction and the macroscopic-microscopic approach with an average Woods-Saxon potential and a monopole pairing interaction are used by S. Cwiok et al, [8] to investigate the ground-state properties of the superheavy elements (SHE) with $108 \leq Z \leq 128$ and $150 \leq N \leq 192$. Rafelski et al., [9] observed that the energy eigenvalues and wave

functions of atomic electrons bound to superheavy nuclei diverge dramatically when the electric field strength is limited. Samanta et al., [10] theoretically estimated alpha-decay half-lives of 314 heavy and superheavy elements in the region $Z = 102-120$ in the WKB frame work with DDM3Y interaction. Aritomo et al., [11] applied the Smoluchowski equation to study the fusion-fission process in heavy systems, with the finite-range droplet model potential.

Oganessian et al., [12] has explained the nuclear stability with $Z=114$ and 184 . The Coulomb and proximity potential models for deformed nuclei (CPPMDN) [13] are used to compute alpha-decay half-lives. Poenaru et al., [14] investigated heavy particle radioactivity with $Z_c > 28$. The UD, UNIV, Horoi, and UDL formulae were used by Zhang and Wang [15] investigated cluster radioactivity of $^{294}118$, $^{296}120$, and $^{298}122$. Warda et al., [16] used a microscopic theory to study the disintegration in heavier nuclei up to Lv ($Z=116$). Using CPPM and CPPMDN [17], alpha-decay half-lives of SHN $Z=122$ are theoretically studied. The macroscopic-microscopic model [18] for the ^{24}Ne emission from ^{232}U is used to calculate the dynamical path for cluster decay. For superheavy nuclei with atomic numbers between 104 and 130, Manjunatha et al., [20] developed a semi-empirical formula for alpha decay half-lives and cluster decay half-lives and compared the logarithmic half-lives generated by the current formula to those obtained from other equations such as the universal decay law (UDL). Earlier researchers [20-34] were used different models such as modified generalized liquid drop model, Coulomb and proximity potential model, effective liquid drop model and different decay modes such as alpha, cluster, proton, beta-decay and spontaneous fission. Literature survey shows inadequate theoretical studies on cluster radioactivity of Maseovium ($Z=115$). Hence in the present work, we have studied cluster radioactivity of ^{287}Mc using modified generalized liquid drop model and various versions of nuclear potential.

2. THEORETICAL FRAMEWORK

The total energy of the system including volume (E_V), surface (E_S), Coulomb (E_C), proximity ($E_{P_{rox}}$) and centrifugal energies (E_l) are given by;

$$E = E_V + E_S + E_C + E_{P_{rox}} + E_l \tag{1}$$

For compound nuclei, the volume, surface and coulomb energies are given by

$$E_V = -15.494(1 - 1.8I^2)A \text{ MeV} \tag{2}$$

$$E_S = 17.9439(1 - 2.6I^2)A^{2/3}(S/4\pi R_0^2) \text{ MeV} \tag{3}$$

$$E_C = 0.6e^2(Z^2/R_0) \times 0.5 \int (V(\theta)/V_0)(R(\theta)/R_0)^3 \sin \theta d\theta \tag{4}$$

where $I, S, V(\theta)$ and V_0 are with usual notations as explained in the literature [35]. When the nuclei are far apart, the equations (2-4) can be expressed as;

$$E_V = -15.494[(1 - 1.8I_1^2)A_1 + (1 - 1.8I_2^2)A_2] \text{ MeV} \tag{5}$$

$$E_S = 17.9439[(1 - 2.6I_1^2)A_1^{2/3} + (1 - 2.6I_2^2)A_2^{2/3}] \text{ MeV} \tag{6}$$

$$E_C = 0.6e^2 Z_1^2/R_1 + 0.6e^2 Z_2^2/R_2 + e^2 Z_1 Z_2/r \tag{7}$$

Here A_i is the mass number, Z_i is the atomic number, R_i is the radii of the two nuclei and I_i is the relative neutron excess of the two nuclei. The radii R_i is determined by;

$$R_i = (1.28A_i^{1/3} - 0.76 + 0.8A_i^{-1/3}) \text{ fm}, i = 1, 2 \tag{8}$$

In the equation (1) the centrifugal energy E_l of the emitted nuclei is expressed as;

$$E_l(r) = \frac{\hbar^2 l(l+1)}{2\mu r^2} \tag{9}$$

Where $\hbar = \frac{h}{2\pi}$. The μ, r and l are the reduced mass, distance between the mass centers of the two nuclei and angular momentum respectively.

The nuclear proximity function Danisov [36] is defined as;

$$V_P(r) = -1.989843 \frac{R_1 R_2}{R_1 + R_2} \varphi(r - R_1 - R_2 - 2.65) \times \left[1 + 0.003525139 \left(\frac{A_1}{A_2} + \frac{A_2}{A_1} \right)^{3/2} - 0.4113263(A_1 + I_2) \right] \tag{10}$$

where the effective nuclear radius is expressed as;

$$R_i = R_{ip} \left(1 - \frac{11.65415}{R_{ip}} \right) + 1.284589 \left(I_i - \frac{0.4A_i}{A_i + 200} \right) (i = 1, 2) \tag{11}$$

where R_{ip} is studied using the relation;

$$R_{ip} = 1.24A_i^{3/2} \left[1 + \frac{1.646}{A_i} - 0.19I \left(\frac{A_i - 2Z_i}{A_i} \right) \right] \text{ with } I_i = \frac{N_i - Z_i}{A_i} \tag{12}$$

The universal function is expressed as;

$$\varphi(s) = \begin{cases} 1 - S(0.7881663 + 1.229218S^2 - 0.2234277S^3 - 0.1038769S^4) - \frac{R_1 R_2}{R_1 + R_2} (0.1844935S^2 + 0.07570101S^3) + (I_1 + I_2) (0.04470645S^2 + 0.03346870S^3) & \text{for } -5.65 \leq S \leq 0 \\ 1 - S^2 \left[0.05410106 \frac{R_1 R_2}{R_1 + R_2} \exp\left(-\frac{S}{1.760580}\right) \right] & \\ -0.5395420 (I_1 + I_2) \exp\left(-\frac{S}{2.424408}\right) \times \exp\left(-\frac{S}{0.7881663}\right) & \text{for } S \geq 0 \end{cases} \tag{13}$$

where $s = r - R_1 - R_2 - 2.65$ is the separation between the two nuclei. Similarly, the nuclear potentials are evaluated using different potentials such as Bass73, AW-91 and BW-91 were studied as explained in detail in reference [37].

The barrier penetration probability is expressed as;

$$P = \exp\left[-\frac{2}{\hbar} \int_{R_n}^{R_{out}} \sqrt{2B(r)(E(r) - E(sphere))} dr\right] \tag{14}$$

Where $R_{in} = R_d + R_\alpha$ and $B(r) = \mu$ is the reduced mass and $R_{out} = e^2 Z_d Z_\alpha / Q_\alpha$. The decay half-life is defined as;

$$T_{1/2} = \frac{\ln 2}{\lambda} = \frac{\ln 2}{\nu_0 P} \quad (15)$$

here ν_0 is the assault frequency and whose value is 10^{20}S^{-1} and P is the barrier penetration probability evaluated using the equation (14).

3. RESULTS AND DISCUSSION

The total potential is evaluated for different possible cluster emissions from the superheavy nuclei ^{287}Mc using the theory explained in the section II.

The Fig. 1 gives the plots of scattering potential versus mass number of cluster emission A_1 in from the superheavy nuclei ^{287}Mc using different proximity functions such as Denisov, BW91, AW91 and Bass73. The variation of scattering potential is minimum for the cluster radioactivity of $^8\text{Be} + ^{279}\text{Rg}$, $^{16}\text{O} + ^{271}\text{Bh}$,

$^{31}\text{P} + ^{254}\text{Fm}$, $^{44}\text{Ca} + ^{243}\text{Am}$, $^{50}\text{Ti} + ^{237}\text{Np}$, $^{64}\text{Ni} + ^{223}\text{Fr}$, $^{74}\text{Ge} + ^{213}\text{Bi}$ using different proximity potentials with the mass number of one of the fragments for ^{287}Mc is observed. Scattering potential is highest for the cluster $^{31}\text{P} + ^{254}\text{Fm}$ and it is lowest for the clusters with magic numbers that is $^8\text{Be} + ^{279}\text{Rg}$ and $^{74}\text{Ge} + ^{213}\text{Bi}$. The graphical representation of scattering potential is useful to analyze the half-life values for the emitted clusters.

The variation of penetration probability with the mass number of one of the fragments for ^{287}Mc for different proximity functions is shown in Fig. 2. From this Fig. it is found that penetration probability is inversely proportional to logarithmic half lives for the emitted clusters. Penetration probability is small for the emitted cluster $^{31}\text{P} + ^{254}\text{Fm}$ and high for the cluster $^{74}\text{Ge} + ^{213}\text{Bi}$ for all the proximity functions. Similar variation will be found for decay constant for all the emitted clusters and it is presented in Fig. 3.

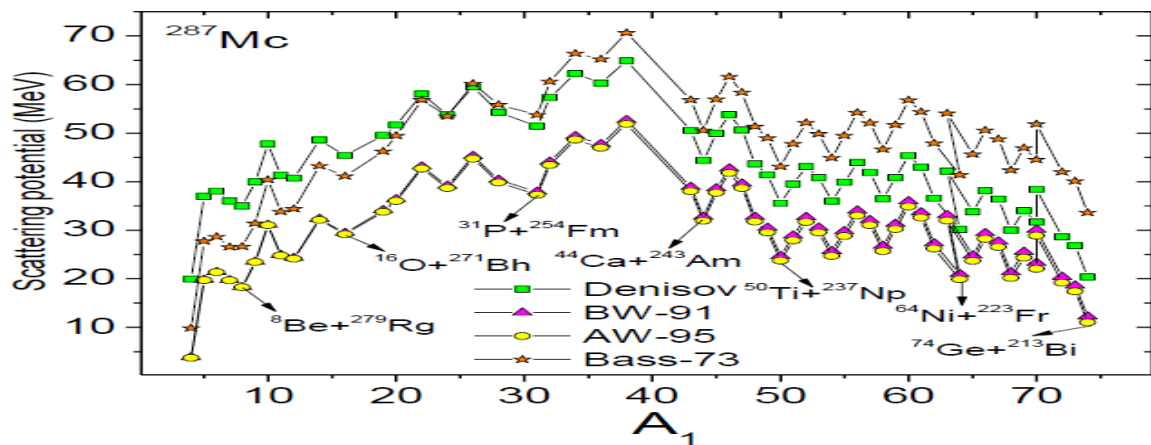


Fig. 1: The scattering potentials as a function of the mass number of one of the fragments for ^{287}Mc for different proximity functions

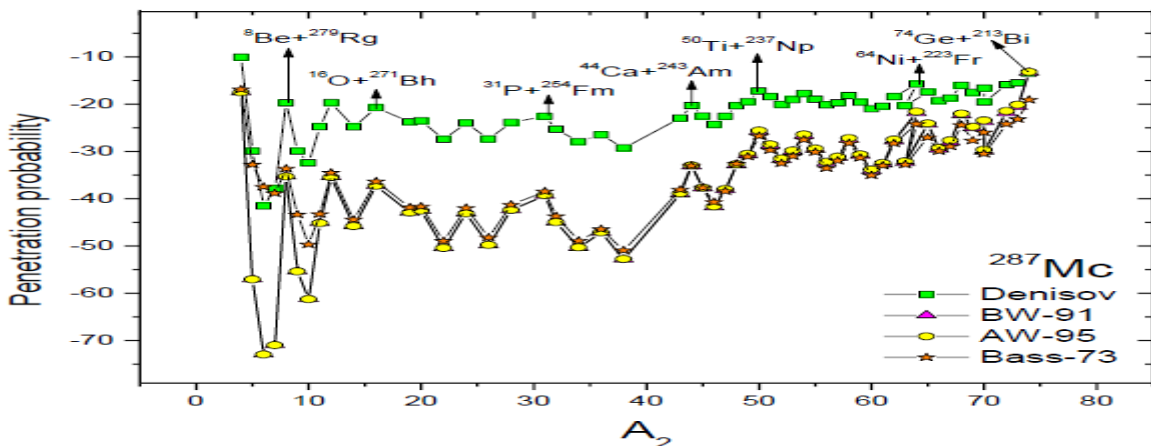


Fig. 2: The penetration probability as a function of the mass number of one of the fragments for ^{287}Mc for different proximity functions.

The variation of logarithmic half-lives with the mass number of one of the fragments for ^{287}Mc for different proximity functions is shown in Fig. 4. From this variation it is found that logarithmic half-life is more for

the cluster $^{31}\text{P}+^{254}\text{Fm}$ and small for the cluster $^{74}\text{Ge}+^{213}\text{Bi}$ for all the proximity functions. These results are due to the presence of magic nuclei in the daughter nuclei.

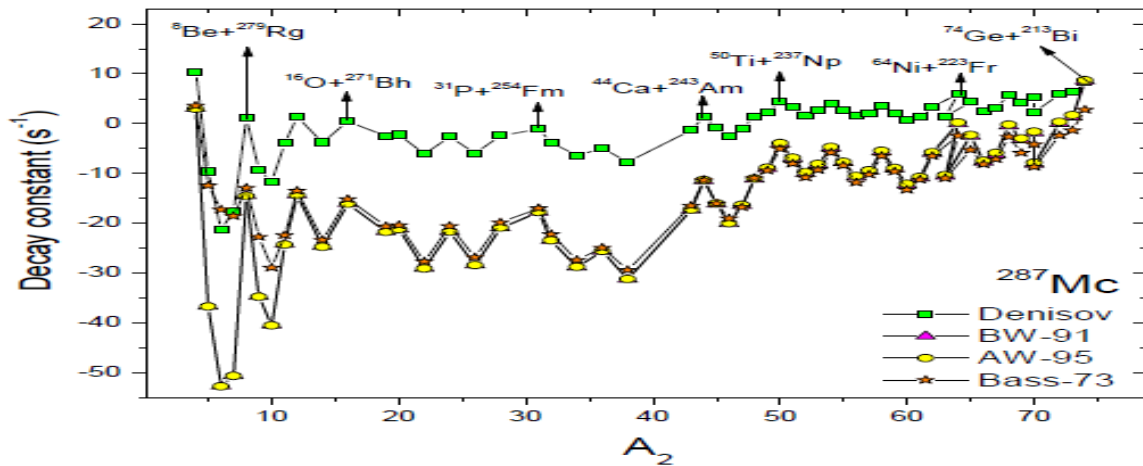


Fig. 3: The decay constant as a function of the mass number of one of the fragments for ^{287}Mc for different proximity functions

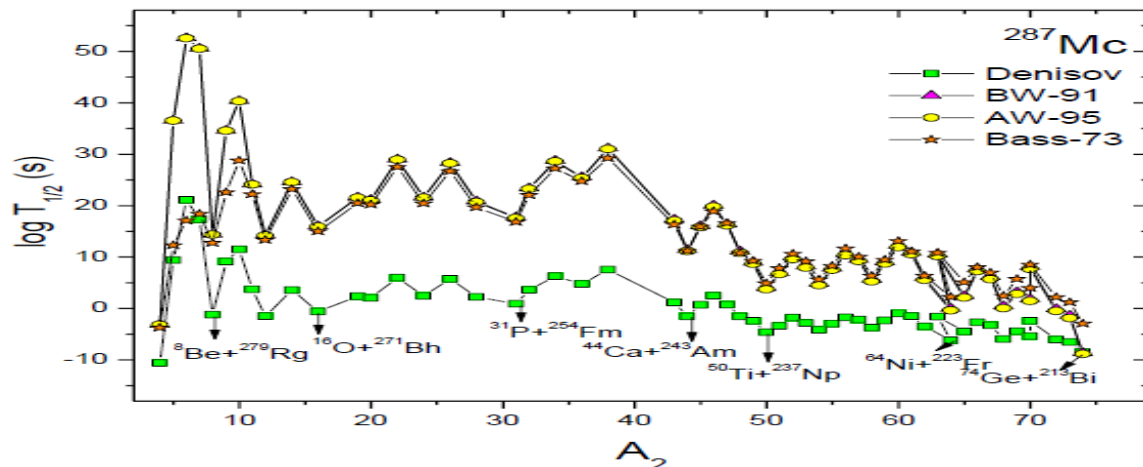


Fig. 4: The logarithmic half-lives as a function of the mass number of one of the fragments for ^{287}Mc for different proximity functions.

4. CONCLUSION

The cluster radioactivity of all cluster emissions were investigated using MGLDM and different nuclear potentials in superheavy nuclei ^{287}Mc . The studied different nuclear potentials such as Danisov, AW-91, BW-91 and Bass-73 shows shorter half-lives and larger relative yield for the cluster emission ^{74}Ge . The logarithmic half-lives corresponding to daughter nuclei $Z=83$ shows shorter half-lives and larger relative yield when compared to other different combinations studied. Hence, the possible cluster decay is with the $^{74}\text{Ge}+^{213}\text{Bi}$.

5. REFERENCES

1. Denisov VY, Hofmann S. *Phys Rev C*, 2000; **61**:034606.
2. Brodziński W, Skalski J. *Phys Rev C*, 2013; **88**:044307.
3. Wei K, Zhang HF. *Phys Rev C*, 2020; **102**: 034318.
4. Takatoshi I. *Phys Rev C*, 2005; **71**:044608.
5. Yury T, Oganessian. *Pure Appl Chem*, 2004; **76**:1715.
6. Carmel Vigila Bai GM, Revathi R. *First ICAPSM IOP*, 2020; **1706**:012021.

7. Poenaru DN, Gherghescu RA. *J Nucl.Phys Mat Sci.Rad A*, 2020; **8**:65.
8. Cwiok S, Dobaczewskia J, Heenen PH, Magierski P, Nazarewicz W. *Nuclear Physics A*, 1996; **611**:211.
9. Rafelski J, Lewis P, Fulcher, Greiner W. *Phys Rev Lett*, 1971; **27**:958.
10. Samantaa C, Roy Chowdhury P, Basu DN. *Nucl Phys A*, 2007; **789**:142-154.
11. Aritomo Y, Wada T, Ohta M. *Phys Rev C*, 1977; **55**:3.
12. Oganessian Y. *Pure Appl. Chem*, 2006; **78**: 889–904.
13. Santhosh KP, Nithya. C. *Phys Rev C*, 2016; **94**:054621.
14. Poenaru DN, Gherghescu RA, Greiner W. *Phys Rev C*, 2012; **85**: 034615.
15. Zhang YL, Wang YZ. *Phys Rev C*, 2018; **97**: 014318.
16. Warda M. Zdeb A., Robledo LM. *Phys Rev C*, 2018; **98**:041602.
17. Manjunatha HC. *Int J Mod Phys E*, 2016; **25**:1650100.
18. Mirea M, Săndulescu A, Delion DS. *Proc Rom Acad A*, 2011; **12**:203-208.
19. Manjunatha HC, Sowmya N, Nagaraja AM. *Mod Phys Lett A*, 2020; **35**: 2050016.
20. Zagrebaev VI, Karpov AV, Greiner W. *Phys Rev C*, 2010; **81**: 044608.
21. Vijayaraghavan KR, Balasubramaniam M, Oertzen WV. *Phys Rev C*, 2015; **91**: 044616.
22. Diehl H, Greiner W. *Nucl Phys A*, 1974; **229**: 29-46.
23. Manjunatha HC, Sowmya N, *Nucl Phys A*, 2018; **969**:68-82.
24. Manjunatha HC, Sowmya N, *Int J Mod Phys E*, 2018; **27**:1850041.
25. Manjunatha HC, Sridhar KN, Sowmya N. *Phys Rev C*, 2018; **98**:024308.
26. Sowmya N, Manjunatha HC. *Bulg J Phys*, 2019; **46**:16-27.
27. Manjunatha HC, Sowmya N, Sridhar KN, Seenappa L. *J Radioanal Nucl Chem*, 2017; **314**:991-999.
28. Sowmya N, Manjunatha HC, Dhananjaya N. *J Radioanal Nucl Chem*, 2020; **323**:1347-1351.
29. Sowmya N, Manjunatha HC. *Braz J Phys*, 2019; **49**:874.
30. Sowmya N, Manjunatha HC. *Braz J Phys*, 2020; **50**:317.
31. Srinivas MG, Manjunatha HC, Sridhar KN, Sowmya N, Raj AC. *Nucl Phys A*, 2020; **995**:1216.
32. Sridhar GR, Manjunatha, HC, Sowmya N, Gupta PSD, Ramalingam HB. *Eur Phys. J Plus*, 2020; **135**:291.
33. Sowmya N, Manjunatha HC. *Phys of Part and Nucl Lett*, 2020; **17**:370.
34. Sridhar GR, Manjunatha, HC, Gupta PSD, Ramalingam HB. *Indian J Pure Appl.Phys.* 2020; **58**:234-240.
35. Manjunatha HC, Sowmya, N. Manjunath N, Seenappa L. *Int J Mod Phys E*, 2020; **29**:2050028.
36. Denisov VY. *Phys.Lett B*, 2002; **526**:315.
37. Zhang GL, Yao YJ. Guo MF, Pan M. *Nucl Phys A*, 2016; **951**:86-96.